Available online at www.sciencedirect.com
ScienceDirect
Catalysis Today 133–135 (2008) 282–291
CATALYSIS TODAY
www.elsevier.com/locate/cattod

Effect of Mo and Co loading in HDS catalysts supported on solvo-thermally treated ZrO_2–TiO_2 mixed oxides

José Escobar [a,*], María C. Barrera [a,b], José A. De Los Reyes [b], María A. Cortés [a], Víctor Santes [c], Elizabeth Gómez [d], José G. Pacheco [e]

[a] *Instituto Mexicano del Petróleo, Prog. de Ing. Molecular, Eje Central Lázaro Cárdenas 152, Col. San Bartolo Atepehuacan, Gustavo A. Madero, México, D.F. 07730, Mexico*
[b] *Universidad Autónoma Metropolitana-Iztapalapa, San Rafael Atlixco 186, Col. Vicentina, Iztapalapa, México, D.F. 09340, Mexico*
[c] *CIIEMAD-IPN, Calle 30 de Junio de 1520, Col. Barrio la Laguna Ticomán, Gustavo A. Madero, México, D.F. 07340, Mexico*
[d] *Instituto de Química-UNAM, Circuito Exterior, Ciudad Universitaria, México, D.F. 04510, Mexico*
[e] *División Académica de Ciencias Básicas, Universidad Juárez Autónoma de Tabasco, Km. 1, Carretera Cunduacán-Jalpa de Méndez, Cunduacán, Tabasco, Mexico*

Available online 1 February 2008

Abstract

Molybdenum (at 2.8, 3.3, 4.0 and 4.7 atoms nm^{-2}) and cobalt (Co/(Co + Mo) ratios of 0.3, 0.4 and 0.5) were impregnated on wide-pore ZrO_2–TiO_2 mixed oxides (30–70) prepared with solvo-thermal treatment (80 °C, 1 day). Materials characterization comprised N_2 physisorption, XRD, thermal analyses, and UV–vis DRS, Raman, and IR spectroscopies. For impregnated dried materials (non-calcined) at concentrations beyond 3.3 atom nm^{-2} and activated by sulfiding (H_2S/H_2, 400 °C) no further improvement in activity in dibenzothiophene (DBT) hydrodesulfurization (HDS) (at 5.59 MPa, T = 320 °C) was observed. Thus, monolayer Mo dispersion was assumed at that content. The aforementioned formulation was chosen to be promoted by Co at different concentrations, the maximum HDS activity being found for sulfided catalyst with Co/(Co + Mo) = 0.4. Nevertheless, the promotion observed by Co addition was small (by a factor of ∼3.2). The activity trends observed in the DBT HDS were well confirmed in the hydrotreatment of a real feedstock (straight-run gasoil). Dibenzothiophene reliably represented the behavior of organo-sulfur compounds present in the middle distillate, at the reaction conditions used in this study where sterically hindered compounds remained unreacted in the hydrotreated gasoil.

Keywords: ZrO_2–TiO_2; Hydrodesulfurization; CoMo catalyst; Dibenzothiophene; Straight-run gasoil

1. Introduction

In recent years, numerous investigations on the production of environmentally friendly cleaner fuels of very low S content have been carried out. Hydrotreatment (HDT) has become a key process in refining schemes focused in getting the aforementioned goal. One of the strategies followed to improve HDT catalyst consists in the development of novel carriers that could impart enhanced activity, selectivity or stability to supported sulfided CoMo or NiMo active phases.

Recently, our group has shown the suitability of solvo-thermal post-treatments during sol–gel processing in improving textural properties of ZrO_2–TiO_2 mixed oxides applied as MoS_2 catalyst support [1,2]. At our best knowledge, these have been the only published works on the application of that methodology to produce wide-pore zirconia–titania. The high-pore volume of that support could make possible to use less concentrated Mo solutions to get a given target loading during impregnation then favoring improved dispersion [3]. In addition, the wide pores present could facilitate diffusion of hydrocarbons constituting middle distillates at HDT conditions. Even more, they could contribute in avoiding rapid deactivation due to partial pore-plugging by carbonaceous deposits, as indeed observed for thiophene HDS over CoMo/TiO_2–ZrO_2 catalysts with pores in the 4–4.5 nm range [4].

In one previous work [1] we reported the high potential of that mixed oxide solvo-thermally treated as MoS_2 catalysts support. Two Mo loadings (2.8 and 5.6 atom nm^{-2}) were tried

* Corresponding author. Tel.: +52 55 9175 8389; fax: +52 55 9175 6380.
E-mail address: jeaguila@imp.mx (J. Escobar).

0920-5861/$ – see front matter
doi:10.1016/j.cattod.2007.12.051

in that investigation where we found decreased HDS activity for formulations of high Mo concentration. Nevertheless, intermediate Mo loadings were not evaluated during that study making difficult to reach conclusions about the optimal value of supported molybdenum concentration, in order to obtain catalysts of maximized HDS activity.

In continuing with our interest in the use of wide-pore ZrO_2–TiO_2 (solvo-thermally treated during 1 day) as HDS catalyst carrier, hereby we present one study focusing on optimizing Mo and Co loadings in order to obtain sulfided catalysts of enhanced hydrodesulfurizating properties. Materials characterization comprised N_2 physisorption, X-ray diffraction, and UV–vis, Raman, and infra-red spectroscopies. The catalytic activity of sulfided Mo and CoMo/ZrO_2–TiO_2 at various impregnated phase concentrations was tested in both HDS of model molecule (DBT) and HDT of a real feedstock (straight-run gasoil, SRGO) from a Mexican refinery. The performance of selected promoted and unpromoted catalysts samples in the hydrodenitrogenation (HDN) of this middle distillate is also reported.

2. Experimental

2.1. Materials synthesis

ZrO_2–TiO_2 (ZT, 30–70 mol-mol) was synthesized by low-temperature sol–gel method followed by solvo-thermal treatment [1]. Zr(IV) propoxide and Ti(IV) isopropoxide (both from Aldrich) were diluted in isopropanol (ROH, Baker). A deionized H_2O + HNO_3 (Baker) mixture was drop-wise added to the alkoxides solution kept under vigorous stirring at ∼0 °C (T_s). The ROH/alkoxides, H_2O/alkoxides and HNO_3/alkoxides mol ratios used were 65, 20 and 0.05, respectively. After alkoxide hydrolysis, the resulting alcogels submerged in the mother liquor were brought to a stainless steel hermetic autoclave (Parr 4560) and treated at 80 °C per 1 day under autogenic pressure. After this stage, the materials were vacuum-dried until total solvent elimination, treated at 120 °C (2 h) and finally calcined at 500 °C (5 h) under static air atmosphere. In the last two thermal treatments a heating ramp of 3 °C min^{-1} was used.

Calcined supports were impregnated at incipient wetness with $(NH_4)_6Mo_7O_{24}{\cdot}4H_2O$ (Aldrich) at various Mo loadings: 2.8, 3.3, 4.0 and 4.7 atoms nm^{-2} (samples M1, M2, M3 and M4, respectively). These impregnated materials were dried at 120 °C (5 h) after aging at room temperature (overnight). No calcining was carried out at this point. Final catalysts were obtained by ex situ sulfiding at 400 °C (1 h) in a flow reactor under a H_2S/H_2 stream (Praxair, 15/85% vol./vol., 4 L h^{-1}). Dried impregnated precursors were first brought to 400 °C (at 10 °C min^{-1}) under N_2 flow (4 L h^{-1}). These conditions were maintained by 3 h. After that period of time, the inert gas flow was switched to the H_2S/H_2 mixture.

To evaluate the effect of promoter concentration, Co at various loadings was added to the M2 dried impregnated precursor, the one that showed the highest HDS intrinsic activity after sulfidation. Three different Co/(Co + Mo) ratios were studied, namely 0.3, 0.4 y 0.5 (samples CM23, CM24 and CM25, respectively). Impregnation at incipient wetness with a $Co(CH_3COO)_2{\cdot}4H_2O$ solution was utilized to this end. The impregnated materials were dried at 120 °C (5 h) after aging at room temperature (overnight), then activated by sulfiding at the aforementioned conditions.

2.2. Materials characterization

N_2 physisorption at −196 °C (Autosorb Quantachrome) was used for textural characterization of studied solids. Materials structural order was studied by X-ray diffraction (Siemens D-500 Kristalloflex, Cu Kα radiation, λ = 0.15406 nm). UV–vis absorption spectra, in powders, were obtained by an Ocean Optics USB2000 miniature optic fiber spectrometer. Raman spectra of support and impregnated materials were measured at room temperature using a Jobin Yvon Inc. Horiba T64000 spectrometer, equipped with a confocal microscope (Olympus, BX41) with the 514.5 nm line from Ar^+ laser (5 mW). Diffuse reflectance infrared Fourier transform spectroscopy (DRIFTS) was applied to study the carrier and Mo impregnated materials by using a Bruker TENSOR 27 spectrometer. After diluting with KBr, materials to be characterized were placed in a sample cup inside the diffuse reflectance unit. Spectra were averaged over 40 scans in the 210–4000 cm^{-1} range, to a nominal 4 cm^{-1} resolution. Spectra are presented in the Kubelká-Munk function format.

2.3. Reaction tests

2.3.1. Dibenzothiophene hydrodesulfurization

Sulfided catalysts were tested in dibenzothiophene (DBT, Aldrich, 98 mass%) hydrodesulfurization (HDS) in a slurry batch reactor (Parr 4562 M), using *n*-hexadecane (Aldrich, 99 + mass%) as solvent. The reaction mixture was prepared by dissolving ∼0.3 g of DBT in 100 cm^3 of *n*-hexadecane and adding ∼0.2 g of sieved catalyst (80–100 Tyler mesh, 0.165 mm average particle diameter). Operating conditions were carefully chosen to avoid external and/or internal diffusional limitations: $P = 5.59 \pm 0.03$ MPa, $T = 320 \pm 2$ °C and 1000 rpm (∼105 rad s^{-1}) mixing speed. Samples taken periodically were analyzed in a gas chromatograph Perkin Elmer AutoSystem XL (flame ionization detector and Econo-Cap-5 capillary column (Alltech). HDS kinetic constants were calculated assuming pseudo-first order kinetics referred to DBT concentration (x = conversion, t = time):

$$k_{\mathrm{HDSDBT}} = \frac{-\ln(1-x)}{t} \quad \text{(I)}$$

k_{HDSBT} values were normalized by considering reaction volume and mass of catalyst used (k_{HDSBT} expressed in m^3 kg_{cat}^{-1} s^{-1}).

2.3.2. Straight-run gasoil (SRGO) hydrotreatment

A real feedstock (SRGO) from a Mexican refinery was also used during catalytic evaluations in a batch reactor (Parr 4571 M). Characteristics of that real feedstock are given in Table 1. Two hundred milliliters of gasoil + 0.5 g of catalyst

Table 1
Properties of the Mexican straight-run gasoil used during HDS and HDN activity tests over sulfided Mo and CoMo catalysts with wide-pore ZrO_2–TiO_2 carrier

Property		Method
IBP[a] (°C)	214.8	ASTM D-86
20%V (°C)	265.6	
40%V (°C)	282.7	
60%V (°C)	301.9	
80%V (°C)	327.2	
FBP[b] (°C)	376.5	
Specific weight 20/4 (°C/°C)	0.8507	ASTM D-4052
S (wt%)	1.222	ASTM D-4294
Total *N* (ppm)	263	ASTM D-4629
Basic *N* (ppm)	107	UOP-313
Aromatics (wt%)	31.7	ASTM D-5186
Monoaromatics	14.4	
Diaromatics	12.8	
Polyaromatics	4.5	
Cetane index	51.7	ASTM D-976

[a] Initial boiling point.
[b] Final boiling point.

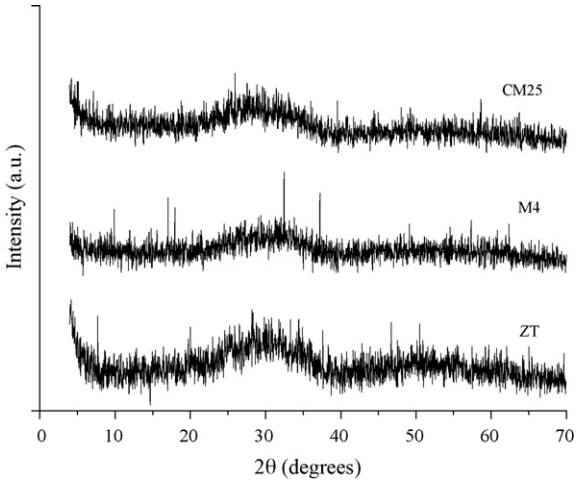

Fig. 1. X-ray diffraction patterns of wide-pore ZrO_2–TiO_2 carrier calcined at 500 °C (ZT) and the corresponding precursors impregnated at the highest metal loadings used. M4: Mo at 4.7 atom nm^{-2}; CM25: Mo at 3.3 atom nm^{-2}, Co/(Co + Mo) = 0.5.

were put in the reactor vessel. Operating conditions were similar to those used in DBT HDS, excepting temperature which was raised to 350 °C. Total S and N content in the reaction product after 4 h (catalytic run duration) were determined by using a quimiluminiscence detector (Antek-7000). Previously to the corresponding analysis, dissolved H_2S and NH_3 were stripped off from the hydrotreated gasoil by bubbling N_2 (1 h).

A pseudo 1.5 order model respecting total sulfur concentration was used to describe SRGO HDS kinetics [5]:

$$k_{\mathrm{HDSSRGO}} = \left[\frac{1}{S_{\mathrm{p}}^{0.5}} - \frac{1}{S_{\mathrm{F}}^{0.5}}\right]\left(\frac{1}{t}\right) \quad \text{(II)}$$

where k_{HDSSRGO}: pseudo 1.5 order SRGO HDS kinetic constant (ppm $S^{-0.5}$ s^{-1}); S_{P}: sulfur in product (ppm); S_{F}: sulfur in feedstock (ppm); t: reaction time (s); k_{HDSSRGO} values were normalized to mass of catalyst used.

A pseudo-first order in total N concentration was used to describe HDN kinetics [6]:

$$k_{\mathrm{HDNSRGO}}\left[\ln\left(\frac{N_{\mathrm{F}}}{N_{\mathrm{p}}}\right)\right]\left(\frac{1}{t}\right) \quad \text{(III)}$$

where k_{HDNSRGO}: pseudo-first order HDN kinetic constant (h^{-1}); N_{F}: total nitrogen in feedstock (ppm); N_{P}: total nitrogen in product (ppm); t: reaction time (s); k_{HDNSRGO} values were normalized to mass of catalyst used.

3. Results and discussion

3.1. Materials characterization

The amorphous ZrO_2–TiO_2 mixed oxide carrier remained without appreciable structural changes after impregnation with Mo and Co. No reflections due to defined Mo or Co phases were evident in the corresponding X-ray diffractograms even in the solids of the highest loading (Fig. 1), suggesting well-dispersed deposited species. However, highly disordered (thus undetectable to the technique used) poly-molybdates domains could not be ruled out. From Fig. 2, the sol–gel ZrO_2–TiO_2 carrier prepared with solvo-thermal post-treatment showed wide pores, suitable in supports of catalysts to be applied in the HDT of middle distillates [7]. Supported phases integration affected to some extent textural properties of the binary oxide carrier. Surface area and pore volume progressively decreased with increasing Mo concentration (Table 2). Surface area loss after impregnation, defined as the difference between theoretical surface area (S_t, considering deposition of a given mass of non-porous phase) and the actual measured value (S_g) augmented with Mo loading suggesting partial pore-plugging in samples of higher molybdenum content, as also indicated from pore size distributions shown in Fig. 2. From Table 3, the additional

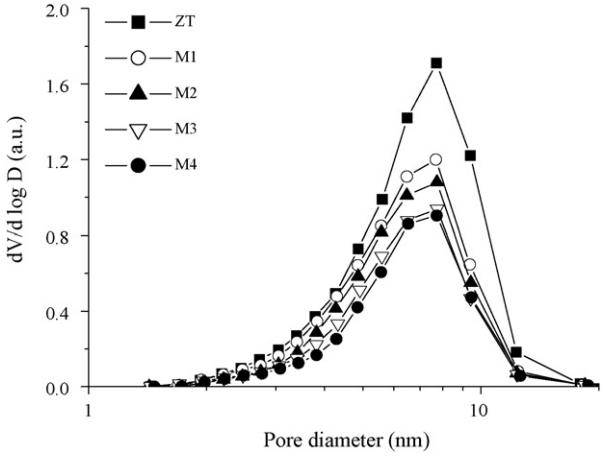

Fig. 2. Pore size distributions of ZrO_2–TiO_2 carrier calcined at 500 °C (ZT) and the corresponding Mo impregnated precursors at various loadings: 2.8, 3.3, 4.0 and 4.7 atoms nm^{-2} (samples M1, M2, M3 and M4, respectively).

Table 2
Textural properties of sol–gel ZrO_2–TiO_2 (30–70) support (calcined at 500 °C) and the corresponding Mo impregnated precursors

Sample	Mo[a] (wt%)	S_g (m^2/g)	S_t (m^2/g)	$100 \times (S_t - S_g)/S_t$ (%)	V_p (cm^3/g)
ZT	–	313	–		0.55
M1	11.9	252	276	8.7	0.40
M2	14.1	216	269	20.0	0.36
M3	16.6	190	261	27.0	0.31
M4	19.0	170	254	33.0	0.28

S_t: theoretical surface area considering deposition of a given mass of non-porous phase.
[a] Nominal Mo content.

texture loss due to Co integration in the M2 precursor was not noticeable.

By UV–vis spectroscopy (Fig. 3), we observed an absorption band intermediate between that of ZrO_2 (insulator) and TiO_2 (semiconductor) in the zirconia–titania support. In the past, we have considered this as evidence of formation of an homogeneous mixed oxide matrix [1]. After impregnation with Mo at various loadings a broad absorption band merged the signal from the support to that of impregnated Mo^{6+}, where oxospecies in octahedral (290–390 nm) coordination [8] could exist. M4 spectrum red-shifted more appreciably than the others, suggesting the presence of Mo species of higher coordination state [9], then of lower dispersion. When Co at different concentrations was incorporated in the dried M2 sample, a band at ~500–700 nm seemed to be due to tetrahedral Co^{2+} [10] (Fig. 4). Slight shoulders at ~410 and ~700 nm (more noticeable for CM23) could be related to octahedral Co^{3+} [11]. Cobalt in those coordinations was identified by Ramírez et al. [10], when characterizing CoMo/TiO_2 materials promoted by fluorine addition. Those species are consistent with the formation of supported Co_3O_4 spinel (which contains two octahedral Co^{3+} ions for one tetrahedral Co^{2+}). It is worth mentioning, however, that other authors [11] have observed this spinel in calcined Co/TiO_2 catalysts just at cobalt loadings higher than 7.6 wt%. Then, certain agglomeration of oxidic cobalt species in our impregnated precursors is suggested. Finally, the artifact registered in the ~638–672 nm range was originated in a detector change (Fig. 4).

The Raman spectrum of the binary oxide matrix (not shown) presented no definite signals due to either titania or zirconia, indicating a highly homogeneous matrix [12]. Samples impregnated with Mo (M1 to M4) then dried, showed a signal

Table 3
Textural properties of M2 impregnated precursor (Mo at 14.1 wt%), after Co addition at various concentrations

Sample	Co (wt%)	S_g (m^2/g)	S_t (m^2/g)	$100 \times (S_t - S_g)/S_t$ (%)	V_p (cm^3/g)
CM23	3.6	205	223	8.1	0.34
CM24	4.2	198	221	10.4	0.31
CM25	4.9	194	220	11.8	0.32

S_t: theoretical surface area considering deposition of a given mass of non-porous phase.

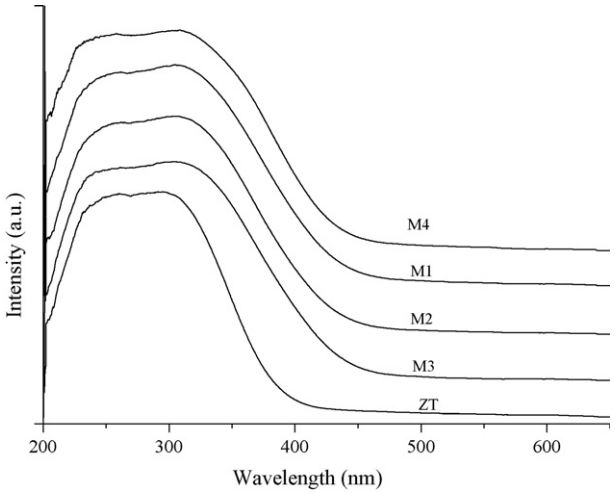

Fig. 3. UV–vis spectra of sol–gel ZrO_2–TiO_2 (30–70 nominal molar ratio) support calcined at 500 °C (ZT) and the corresponding Mo impregnated precursors at various loadings: 2.8, 3.3, 4.0 and 4.7 atoms nm^{-2} (samples M1, M2, M3 and M4, respectively).

centered at ~947 cm^{-1} assigned to Mo=O stretching vibrations of dioxo groups of oxomolybdate species MoO_{2t} (where "t" stands for terminal oxygen atoms) [3] (see Fig. 5). This signal could be originated by deposition of $Mo_7O_{24}^{6-}$ anions present in the slightly acidic (pH ~6–7) ammonium heptamolybdate solution [13]. The intensity of the observed band increased with Mo content in the studied samples but no information about its dispersion could be inferred from these data. Definite domains of MoO_3 were not registered even in the samples of higher molybdenum concentration (see Fig. 5) because our impregnated solids were not submitted to calcining at temperature high enough to provoke tri-dimensional molybdemum oxide formation.

The broad band at ~618–629 cm^{-1} could be formed from contributions of the signal at ~637 cm^{-1} characteristic of anatase titania [3]. It should be noted, however, that due to its very low intensity, this shoulder could not be considered as

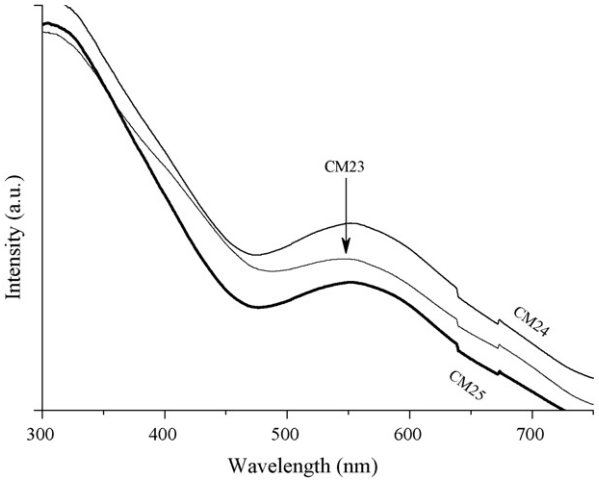

Fig. 4. Visible spectra of CoMo/ZrO_2–TiO_2 impregnated precursors. Mo at 3.3 atom nm^{-2} and cobalt at Co/(Co + Mo) = 0.3, 0.4 and 0.5.

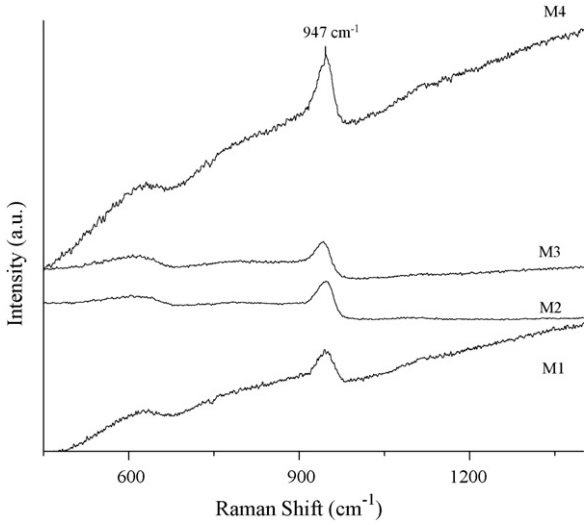

Fig. 5. Raman spectra of Mo impregnated precursors at various loadings: 2.8, 3.3, 4.0 and 4.7 atoms nm^{-2} (samples M1, M2, M3 and M4, respectively).

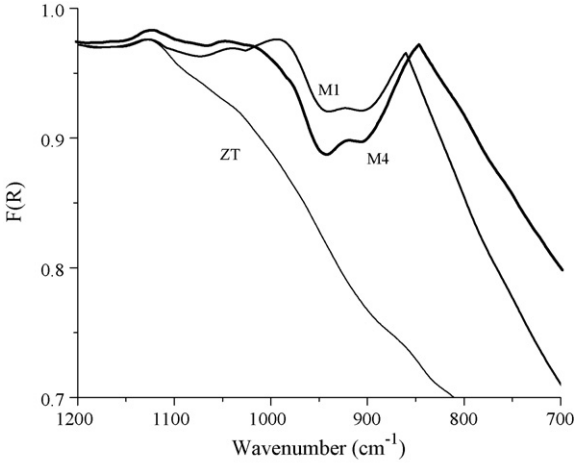

Fig. 7. DRIFT spectra of ZrO_2–TiO_2 carrier and the corresponding Mo impregnated precursors at different loadings: 2.8 and 4.7 atoms nm^{-2} (samples M1 and M4, respectively). Oxo-molybdates absorption zone.

evidence of titania segregation. Indeed, that slight signal is appreciable just at the high magnification that had to be used to distinguish the very small peaks originated by octahedral impregnated Mo [2].

The DRIFT of ZT support did not present any defined band in the frequency region characteristic for titania or zirconia [14] (absorption range not shown) in agreement with the formation of an homogeneous matrix. Upon Mo dispersion onto the carrier surface, the intensity of basic hydroxyl groups bands (3690–3710 cm^{-1}) progressively decreased by augmenting Mo loading (Fig. 6), being this effect more noticeable in sample M4, the one of the highest loading. In this regard, it is well known that molybdate anions preferably interacts with that kind of hydroxyls [15]. Simultaneously, new bands that appeared at 907 and 942 cm^{-1} could be ascribed to deposited poly-molybdates (Fig. 7), the registered absorptions being originated by Mo=O stretching vibrations [16]. The lack of characteristic bands for MoO_3 in the DRIFT spectra of Fig. 7 discards the presence of this crystalline phase, in agreement with our Raman spectroscopy results (Fig. 5). By calcining sample M2 at 400 and 600 °C (by 5 h in air) the bands at 907 and 942 cm^{-1} exhibited a continuous shift to higher wave numbers and become more noticeable at 975 cm^{-1} in the sample calcined at 600 °C (Fig. 8). That band is characteristic of the stretching vibration mode of terminal double bond M=O of crystalline MoO_3 [17]. Thus, by avoiding high-temperature annealing (as part of our catalyst preparation methodology) agglomeration and crystallization of deposited Mo was precluded, providing a better precursor for the formation of dispersed MoS_2 crystallites.

3.2. Activity tests

3.2.1. DBT HDS

M2 and M4 were the sulfided Mo/ZrO_2–TiO_2 catalysts of the highest DBT HDS activity (Fig. 9). However, if the Mo content is taken into account (Table 1), it is clear that the best

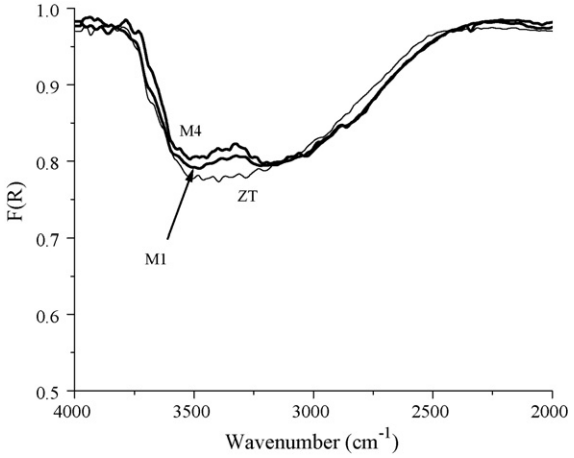

Fig. 6. DRIFT spectra of ZrO_2–TiO_2 carrier and the corresponding Mo impregnated precursors at different loadings: 2.8 and 4.7 atoms nm^{-2} (samples M1 and M4, respectively). Hydroxyl groups absorption zone.

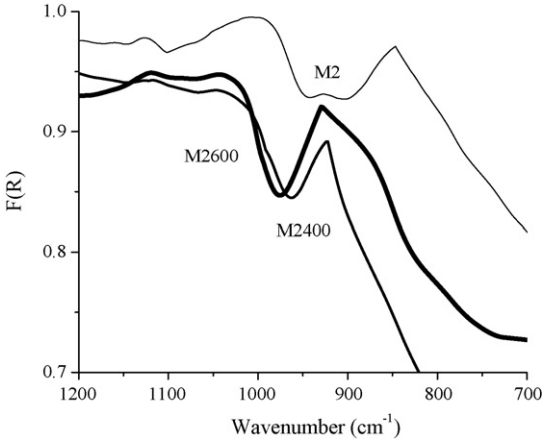

Fig. 8. DRIFT spectra of ZrO_2–TiO_2 carrier and the corresponding Mo impregnated precursors at 3.3 atoms nm^{-2}. M2: dried; M2400: calcined at 400 °C; M2600: calcined at 600 °C. Oxo-molybdates absorption zone.

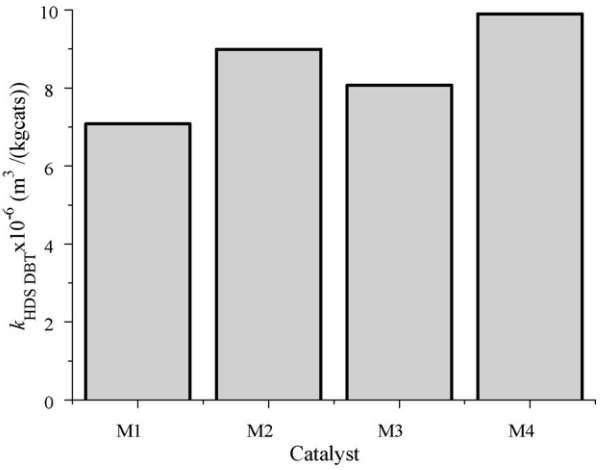

Fig. 9. Pseudo-first order kinetic constants (DBT HDS) of sulfided Mo catalysts supported on solvo-treated ZrO_2–TiO_2. Mo at various loadings: 2.8, 3.3, 4.0 and 4.7 atoms nm^{-2} (samples M1, M2, M3 and M4, respectively). $P = 5.59 \pm 0.03$ MPa, $T = 320 \pm 2$ °C, 1000 rpm (∼105 rad s^{-1}) mixing speed, solvent: *n*-hexadecane.

formulation is the former, as in the latter a molybdenum concentration ∼35% higher than that on M2 is reflected in just ∼10% improvement in hydrodesulfurization activity. This fact suggested that Mo monolayer on our solvo-thermally treated zirconia–titania mixed oxides could be obtained at 3.3 atom nm^{-2}, a value slightly lower to the 4 atom nm^{-2} dispersable over high surface area titania prepared by multi-gelation method [3] where ammonium heptamolybdate at natural solution pH (∼6–7) was impregnated at various loadings. In the latter calcined (500 °C) sample, Vrinat and coworkers [3] registered (by Raman spectroscopy) just the presence of octahedral poly-oxomolybdates but when they deposited higher Mo amounts (5 atom nm^{-2}), definite domains of MoO_3 (signals at 820 and 916 cm^{-1} [3]) were observed indicating lower deposited phase dispersion. Thus, solubility of $Mo_7O_{24}^{6-}$ anions in aqueous solutions results one of the main factors that limit the efficient dispersion of deposited molybdenum. HDS catalytic activity of the corresponding sulfided catalysts could be consequently affected. In our case, it is expected that by increasing the Mo concentration in the impregnating solution the deposited phase were less dispersed.

As aforementioned, the small enhancement (∼10%) in HDS activity observed by augmenting Mo content from 14 to 19 wt% (samples M2 and M4) could be ascribed to monolayer formation. Indeed, Vrinat and coworkers [3] observed a marginal increase in dibenzothiophene conversion by varying Mo concentration on high surface area TiO_2 from 8 to 12 wt% (once that monolayer had been established). They found that the augmented MoS_2 surface concentration in the latter catalyst was not reflected in hydrodesulfurizating activity improvement due to decreased crystals dispersion.

As reference, we impregnated Mo (by using a methodology similar to that used for the samples with ZT carrier and at similar concentration to that of our M2 sample) over a last-generation alumina-based support ($S_g \sim 400$ m^2/g) for commercial catalysts to be applied in the hydrotreatment of middle distillates. In this case, the *k* (pseudo-first order kinetic constant DBT HDS) determined was 4.6×10^{-6} m^3 (kg$_{cat}^{-1}$ s^{-1}), value about 50% lower as to that corresponding to sulfided M2, making evident the potential of using the ZT mixed oxide carrier.

The formulation M2 was chosen to be promoted by different amounts of Co to try to determine the concentration at which cobalt could exert maximized promotion of supported MoS_2 phase. The criterion we followed to utilize the M2 sample for our further study was the higher (∼21%) intrinsic HDS activity (per mass of Mo) that it presented, as to that of the sulfided M4 sample.

From Fig. 10, the most efficient cobalt integration (k_{HDSDBT} increased by a factor of ∼3.2) was found for the catalyst CM24. That activity enhancement by Co addition was much lower to values registered for alumina-supported formulations (∼25) [18]. Wang et al. [18] observed the highest promotion of Mo/TiO_2 by Co at Co/(Co + Mo) = 0.38, for sulfided catalysts tested in the liquid-phase DBT HDS. In this case, the corresponding activity promotion was by a factor of about 3. Similar trends have been previously reported by others regarding CoMo/TiO_2 tested in gas-phase HDS reactions. For instance, Ramírez et al. [19] observed augmented activity in the thiophene hydrodesulfurization (per Mo atom) over both unpromoted and promoted samples, respecting the alumina-supported counterparts, although these showed higher promotion by Co addition. Regarding ZrO_2-supported catalysts, Ji et al. [20] found that sulfided molybdenum was twice as active as Mo/Al_2O_3 in the thiophene HDS but, again, the promotion registered by Co addition was much larger in the latter (∼11.2 *versus* 3.3 in materials with zirconia carrier). Interestingly, the promotion in HDS activity of Mo/ZrO_2–TiO_2 by Co addition, as observed in the present work, seemed to be well correlated to values registered for other authors over sulfided CoMo supported on either titania or zirconia single oxides.

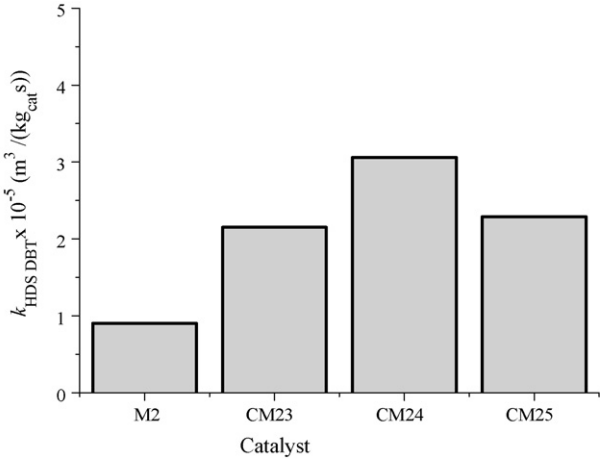

Fig. 10. Pseudo-first order kinetic constants (DBT HDS) of sulfided CoMo catalysts (Mo at 3.3 atom nm^{-2}) supported on solvo-treated ZrO_2–TiO_2 (30–70 nominal molar ratio). Effect of Co/(Co + Mo) ratio. CM2: 0.2, CM3: 0.3, CM4: 0.4. $P = 5.59 \pm 0.03$ MPa, $T = 320 \pm 2$ °C, 1000 rpm (∼105 rad s^{-1}) mixing speed, solvent: *n*-hexadecane.

To try to explain the low promotion of titania-supported sulfided Mo by Co, Wang et al. [18] proposed that due to partial surface sulfidation of the carrier a TiS_2 phase could be formed during activation of the corresponding impregnated precursors. Also, Ti^{4+} cations could be reduced to Ti^{3+}. According to those authors, this species could transfer electrons to the supported molybdenum phase weakening Mo–S bonds because of the formation of a ''TiMoS'' phase (similar to the ''CoMoS'' one) that could increase the electronic density of Mo, thus enhancing the mobility of labile sulfur. In fully agreement with this way of reasoning, Ramírez et al. [21] concluded that TiO_2 is not a ''conventional'' support but also an electronic promoter of the MoS_2, maintaining electronic contact wit this sulfided phase through the conduction band. Even more, they proposed that this fact could limit the effect of Co addition, being the cause of the small to moderate enhancement in HDS activity commonly observed in Mo/TiO_2 by Co integration [22].

A similar phenomenon, due to the influence of titania content, could explain the low promotion of Mo by Co on our titania–zirconia-supported molybdenum sulfide catalysts. It should be noted, however, than differently to the case of the aforementioned investigations in this case no defined anatase titania domains were present (see Fig. 1). In the past, we have observed partial titania sulfidation when studying CoMo catalyst with nano-structured titania as carrier [23], revealing that titanium surface sulfides could be formed under appropriate conditions although TiO_2 is in a different phase to anatase. For a commercial promoted Mo formulation with an Al_2O_3-based support of last generation (Mo, Co and P at 14.2, 3.4 and 1.8 wt%, respectively) the corresponding k registered was of 11.1×10^{-5} m^3 (kg_{cat}^{-1} s^{-1}), value more than threefold higher than that of sulfided CM24, the best ZT-supported CoMo catalyst. The observed activity trend could be determined by a much more efficient promotion of MoS_2 by Co in the catalysts with alumina carrier (by a factor >20). Thus, the necessity of finding methodologies that could allow obtaining high promotion of Mo catalyst by Co integration when supported on titania or its mixed oxides results evident. In this line, recently, some investigators [24] have reported the preparation of CoMo catalyst

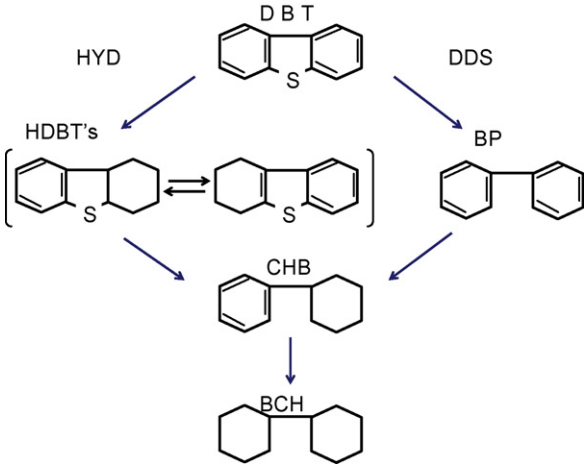

Fig. 11. DBT HDS reaction network over sulfided $CoMo/Al_2O_3$, from [25].

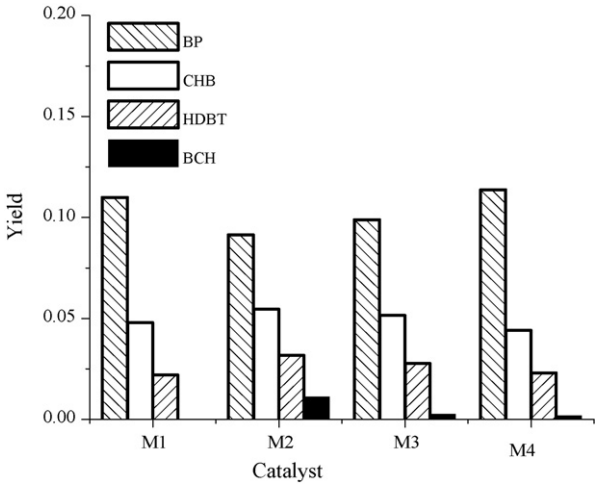

Fig. 12. Yield to different products (DBT HDS at ~18% conversion) of sulfided Mo catalysts at various loadings supported on solvo-treated ZrO_2–TiO_2 (30–70 nominal molar ratio). Mo at: 2.8, 3.3, 4.0 and 4.7 atoms nm^{-2} (samples M1, M2, M3 and M4, respectively). $P = 5.59 \pm 0.03$ MPa, $T = 320 \pm 2$ °C, 1000 rpm (~105 rad s^{-1}) mixing speed, solvent: n-hexadecane.

with anatase titania carrier, which very high activity in the SRGO HDS could be explained by efficient Co–Mo integration.

Fig. 11 is a well-known scheme showing the DBT HDS reaction routes [25]. Although other intermediate products have been considered by other authors [26], we preferred the scheme proposed by Houalla et al. [25] for sake of simplicity. Direct desulfurization (DDS) resulted in biphenyl (BP) meanwhile the hydrogenation path (HYD) produced hexa- and tetra-hydrodibenzothiophenes (HDBT) intermediaries that could be further desulfurized to cyclohexylbenzene (CHB). Considering that BP hydrogenation to CHB could be strongly inhibited by DBT competitive adsorption under HDS conditions [27], we considered that all CHB came from HYD route (Fig. 11). Sulfided M2 had slightly better hydrogenating properties than the rest of supported Mo catalysts (Fig. 12), although BP in all cases was the main product registered. Over that solid, about ~50% of the products (at ~18% conversion) came from the HYD route (HDBT, CHB and bicyclohexyl, BCH). Also, M2 was able to completely saturate certain amounts of CHB to BCH. No cracking products were observed, in agreement with the absence of strong acidity on the binary oxide support [1]. According to Daage and Chianelli model for unsupported catalysts [28], MoS_2 crystallites of low stacking degree (low number of superimposed layers) could favor a higher proportion of active sites (sulfur vacancies in the so-called ''rim sites'') able to transform DBT through the HYD route whereas DDS route (to BP) could be preferably promoted by edge sites which number could be increased in more stacked molybdenum sulfide slabs. Other authors also agree with that concept attributing better hydrogenating properties to promoted MoS_2/Al_2O_3 particles of lower stacking degree [29]. Taking this into account, MoS_2 particles of lower number of stacked layers (thus, with higher number of hydrogenating rim sites) could be preferably found in the sulfided M2 catalyst.

All the Co-promoted M2 sulfided samples showed similar product yield trends one to another (Fig. 13), where BP propor-

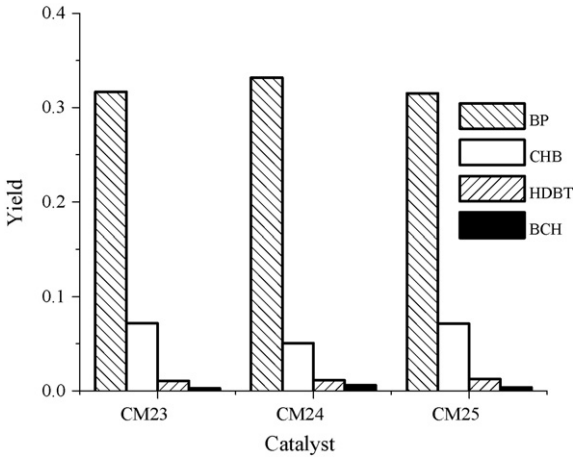

Fig. 13. Yield to different products (DBT HDS at ∼40% conversion) of Co-promoted sulfided Mo catalysts (at 3.3 atom nm^{-2}, Co/(Co + Mo) = 0.4) supported on solvo-treated ZrO_2–TiO_2 (30–70 nominal molar ratio). $P = 5.59 \pm 0.03$ MPa, $T = 320 \pm 2$ °C, 1000 rpm (∼105 rad s^{-1}) mixing speed, solvent: *n*-hexadecane.

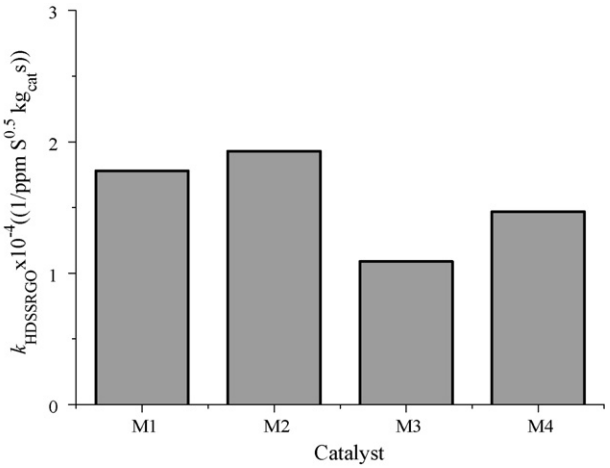

Fig. 14. Pseudo 1.5 order kinetic constants (SRGO HDS) of sulfided Mo catalysts at various loadings supported on solvo-treated ZrO_2–TiO_2 (30–70 nominal molar ratio). Mo at various loadings: 2.8, 3.3, 4.0 and 4.7 atoms nm^{-2} (samples M1, M2, M3 and M4, respectively). $P = 5.59 \pm 0.03$ MPa, $T = 350 \pm 2$ °C, 1000 rpm (∼105 rad s^{-1}) mixing speed.

tion was strongly increased, as to that found for the unpromoted M2 catalyst (Fig. 12). By comparing Figs. 12 and 13 it is clear that the DDS route was much more promoted than the HYD one by Co addition. Other investigators [18] have found similar results when testing unpromoted and promoted (by Ni or Co) MoS_2 supported on TiO_2. Interestingly, for catalysts with alumina carrier Mijoin et al. [26] considered that enhanced amounts of biphenyl from the DDS route in the DBT HDS could be indicative of efficient Co integration to the MoS_2 phase. In this regard, the DDS route could be enhanced by a factor of ∼60 whereas HYD pathway just showed a threefold increase [30].

In agreement with that registered for our CoMo/TiO_2–ZrO_2, other investigators observed enhanced DBT transformation through the DDS path over CoMo/TiO_2 (as to that over the unpromoted phase) although the magnitude of that effect was lower to that determined for alumina-supported catalysts [18]. As already mentioned, the promotion of MoS_2 by Ti (the ''TiMoS'' phase) could be responsible for this less-efficient Co integration. It seems that the behavior of our HDS catalysts supported on titania–zirconia was somehow dictated by the reducibility–sulfidability of titania under the H_2S/H_2 atmosphere that prevails during activation and testing of HDS catalysts, even though characterization of our binary oxide carrier through various techniques (XRD, Raman, IR) evidenced the absence of definite domains of titanium oxide.

3.2.2. SRGO HDT

The activity trends found in DBT HDS over the samples M1–M4 were well correlated with those observed in SRGO HDT (Fig. 14) where M2 was the sulfided catalyst of the highest HDS activity. This meant that DBT HDS was a reliable model test to accurately estimate the performance of Mo/ZrO_2–TiO_2 catalyst in the HDT of real feedstock. It should be taken into account, however, that this could be valid just at conversion levels where refractory, sterically hindered compounds, remained unreacted in the hydrotreated oil (S conversion <95%), as was in the present case. Under these conditions, DBT could represent organo-sulfur compounds present in the used SRGO. In fact, previous analyses showed that DBT and its alkylated derivatives (excluding refractory DBT's with alkyl groups in the 4 and/or 6 positions) constituted about 50 wt% of the S-bearing heterocompounds in this middle distillate. Beyond that conversion level, removal of sterically hindered DBT's takes place. These species need to be previously hydrogenated to be desulfurized, following the HYD route [30] instead of the DDS one preferred for DBT elimination over sulfided CoMo catalysts (see Fig. 11).

Nitrogen compounds present in Mexican gasoils are constituted by quinolines (basic, ∼25 wt%), indoles and carbazoles (non-basic, ∼75 wt%) [31], the former being considered strong inhibitors of HDS reactions [6]. Respecting SRGO hydrodenitrogenation (HDN), again, M2 was the best formulation (the one of the highest intrinsic activity), Fig. 15. Probably, its slightly enhanced hydrogenating properties

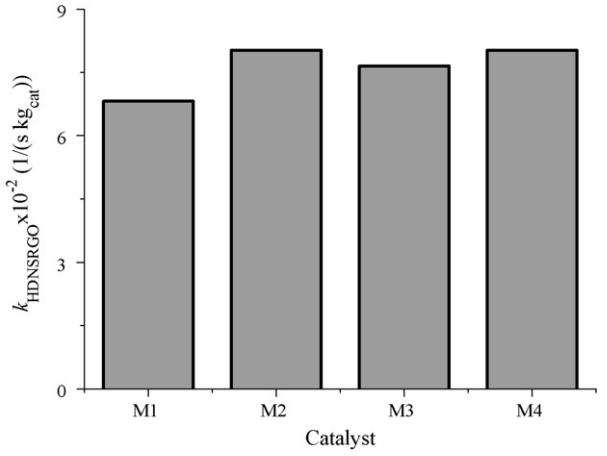

Fig. 15. Pseudo-first order kinetic constants (SRGO HDN) of sulfided Mo catalysts at various loadings supported on solvo-treated ZrO_2–TiO_2 (30–70 nominal molar ratio). Mo at: 2.8, 3.3, 4.0 and 4.7 atoms nm^{-2} (samples M1, M2, M3 and M4, respectively). $P = 5.59 \pm 0.03$ MPa, $T = 350 \pm 2$ °C, 1000 rpm (∼105 rad s^{-1}) mixing speed.

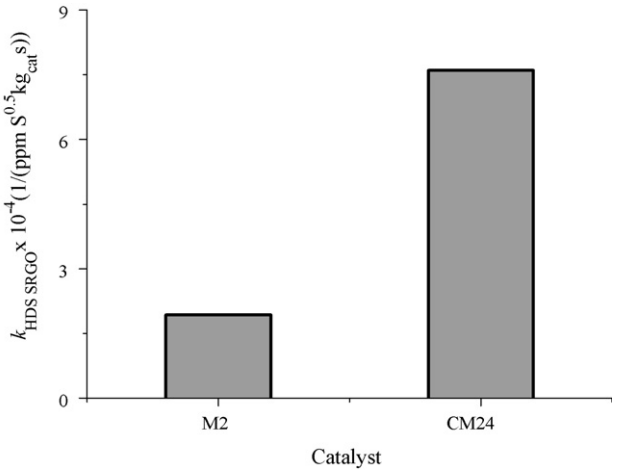

Fig. 16. Pseudo 1.5 order kinetic constants (SRGO HDS) of sulfided Mo (at 3.3 atom nm^{-2}) and the corresponding Co promoted catalysts (Co/(Co + Mo) = 0.4) supported on solvo-treated ZrO_2–TiO_2 (30–70 nominal molar ratio). $P = 5.59 \pm 0.03$ MPa, $T = 350 \pm 2$ °C, 1000 rpm (∼105 rad s^{-1}) mixing speed.

(Fig. 12) could contribute to this behavior, as it is well known that aromatics hydrogenation is a determining step in HDN mechanism [6]. Regarding sulfided CoMo catalysts supported on ternary oxides ZrO_2–TiO_2–V_2O_5, Wang and Chang [32], reported the highest HDN activity (in simultaneous DBT HDS and aniline HDN) at 1.9 Mo atoms nm^{-2}. This discrepancy could be rationalized by considering that the presence of V_2O_5 could strongly modify the surface properties of zirconia–titania binary carriers.

The effect of Co addition at Co/(Co + Mo) = 0.4 on the performance in the SRGO HDS over sulfided M2 is shown in Fig. 16. The promotion observed was of ∼3.9, well correlated to that registered in the DBT HDS test (∼3.2, see Fig. 10). Regarding HDN, the activity of M2 was increased by a factor of ∼2.5 by Co addition at the aforementioned atomic ratio, Fig. 17. This lower promotion in HDN could be due to that

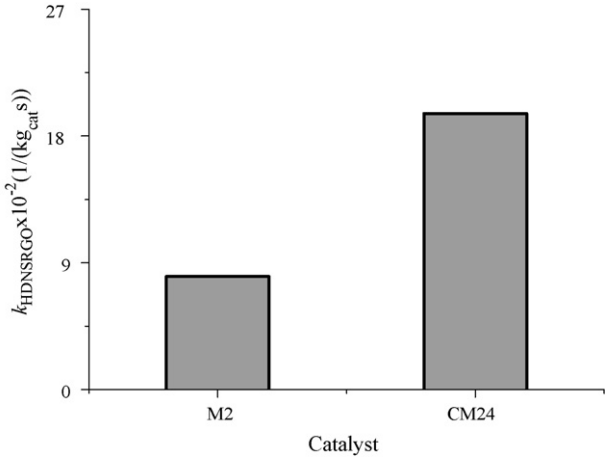

Fig. 17. Pseudo-first order kinetic constants (SRGO HDN) of sulfided Mo (at 3.3 atom nm^{-2}) and the corresponding Co promoted catalysts (Co/(Co + Mo) = 0.4) supported on solvo-treated ZrO_2–TiO_2 (30–70 nominal molar ratio). $P = 5.59 \pm 0.03$ MPa, $T = 350 \pm 2$ °C, 1000 rpm (∼105 rad s^{-1}) mixing speed.

hydrogenating properties were less enhanced than desulfurization ones by cobalt integration, as could be noted by comparing the plots in Figs. 12 and 13. Wang and Chang [32] registered much lower HDS promotion when studying Mo and CoMo formulations with ZrO_2–TiO_2–V_2O_5 carrier, where the optimal Co/(Co + Mo) ratio was of 0.33. They observed a twofold increase in HDS activity when those catalysts were tested in the simultaneous DBT HDS and aniline HDN. During this series of experiments, the HDN enhancement by Co addition on Mo catalyst with zirconia–titania–vanadia carrier was of about 3. In SRGO HDT we found a HDN promotion/HDS promotion ratio of about 0.64, value much lower to that reported by Wang and Chang (∼1.5) [32] from their simultaneous HDS–HDN experiment using a synthetic mixture composed of DBT + aniline dissolved in toluene + mesitylene. Thus, an additional contribution to HDN activity is suggested in the latter. Indeed, those authors proposed that surface acid sites on the ternary support could promote aromatics hydrogenation and C–N bonds breaking that could result in improved aniline HDN. Weissman et al. [33] reached similar conclusions when studying the HDS and HDN of light straight-run gasoil over sulfided NiMo/TiO_2–ZrO_2. In previous investigations by Chang and Wang [34] on the performance of ZrO_2–TiO_2–V_2O_5 ternary oxides in the dehydrogenation and isomerization of cyclohexane a linear relationship between the amount of strong acid sites ($H_o \leq -3.0$, titration with *n*-butylamine) and the activity in those reactions was found. Also, based on their investigations on the naphthalene hydrogenation over Pt/ZrO_2–TiO_2 Lu et al. [35] proposed that acid sites present on the carrier could provide adsorption sites for aromatic molecules, this fact resulting in enhanced ring saturation.

In the opposite to that found in the aforementioned works, previous detailed characterization of our zirconia–titania mixed oxides [1] evidenced absence of strong surface acid sites. Thus, the corresponding sulfided CoMo catalysts could be lacking the contribution of those sites on the hydrogenation of aromatics that, in turn, could influence the HDN properties [6]. That could explain the lower promotion of Mo (by Co addition) in HDN, as to that found for HDS, during our middle distillate hydrotreating experiments.

4. Conclusions

According to dibenzothiophene hydrodesulfurization (at 5.59 MPa, and 320 °C) data, molybdenum monolayer over amorphous wide-pore ZrO_2–TiO_2 (30–70) prepared by sol–gel with solvo-thermal post-treatment (80 °C) seemed to be formed at 3.3 atoms nm^{-2}. At this composition, the sulfided catalysts showed slightly higher yield of hydrogenated products, as compared to the rest of formulations prepared at different Mo loadings. When Co was added at different concentrations to that non-calcined formulation, the maximum in the DBT HDS was found for sulfided catalyst with Co/(Co + Mo) ratio of 0.4. However, even in this case the promotion observed (in a pseudo-first order kinetic constants basis) was rather low (by a factor of ∼3.2). The increase in MoS_2 activity by Co promotion was of similar magnitude in both HDS of dibenzothiophene and

hydrotreatment of a Mexican straight-run gasoil. This fact suggested that the used model molecule reliably represents the organo-sulfur compounds existing in that middle distillate, when the sulfur removal level attained (S conversion <95%) does not involve desulfurization of sterically–hindered DBT's. Hydrodenitrogenation activity over sulfided $CoMo/ZrO_2$–TiO_2 seemed to be limited by the absence of strong acid sites on the binary oxide carrier surface.

Acknowledgements

The authors recognize financial support from Instituto Mexicano del Petróleo and UAM-Iztapalapa. They also appreciate the comments from Dr. M. Vrinat (CNRS) to improve this work.

References

[1] M.C. Barrera, M. Viniegra, J. Escobar, M. Vrinat, J.A. De Los Reyes, F. Murrieta, J. García, Catal. Today 98 (2004) 131.
[2] M.C. Barrera, J. Escobar, J.A. de los Reyes, M. Cortés, M. Viniegra, A. Hernández, Catal. Today 116 (2006) 498.
[3] S. Dzwigaj, C. Louis, M. Breysse, M. Cattenot, V. Bellière, C. Geantet, M. Vrinat, P. Blanchard, E. Payen, S. Inoue, H. Kudo, Y. Yoshimura, Appl. Catal. B 41 (2003) 181.
[4] F.P. Daly, H. Ando, J.L. Schmitt, E.A. Sturm, J. Catal. 108 (1987) 401.
[5] T. Fujikawa, O. Chiyoda, M. Tsukagoshi, K. Idei, S. Takehara, Catal. Today 45 (1998) 307.
[6] M.J. Girgis, B.C. Gates, Ind. Eng. Chem. Res. 30 (1991) 2021.
[7] A.L. Dicks, R.L. Ensell, T.R. Phillips, A.K. Szczepura, M. Thorley, A. Williams, R.D. Wragg, J. Catal. 72 (1981) 266.
[8] L. Mosqueira, G.A. Fuentes, Mol. Phys. 100 (2002) 3055.
[9] R.S. Weber, J. Catal. 151 (1995) 470.
[10] J. Ramírez, R. Cuevas, L. Gasque, M. Vrinat, M. Breysse, Appl. Catal. 71 (1991) 351.
[11] Y. Brik, M. Kacimi, M. Ziyad, F. Bozon-Verduraz, J. Catal. 202 (2001) 118.
[12] J. Miciukiewicz, T. Mang, H. Knözinger, Appl. Catal A 122 (1995) 151.
[13] G. Xiong, Z. Feng, J. Li, Q. Yang, P. Ying, Q. Xin, C. Li, J. Phys. Chem. B 104 (2000) 3581.
[14] M. Daturi, A. Cremona, F. Milella, G. Busca, E. Vogna, J. Eur. Ceram. Soc. 18 (1998) 1079.
[15] N.Y. Topsøe, H. Topsøe, J. Catal. 139 (1993) 631.
[16] C. Martin, I. Martín, V. Rives, P. Malet, J. Catal. 161 (1996) 87.
[17] M. Kassem, Inorg. Mater. 42 (2006) 165.
[18] D. Wang, X. Li, E.W. Qian, A. Ishihara, T. Kabe, Appl. Catal. A 238 (2003) 109.
[19] J. Ramírez, S. Fuentes, G. Díaz, M. Vrinat, M. Breysse, M. Lacroix, Appl. Catal. 52 (1989) 211.
[20] Y. Ji, P. Afanasiev, M. Vrinat, W. Li, C. Li, Appl. Catal. A 257 (2004) 157.
[21] J. Ramírez, L. Cedeño, G. Busca, J. Catal. 184 (1999) 59.
[22] L. Kaluža, D. Gulková, Z. Vít, M. Zdražil, Appl. Catal. A 324 (2007) 30.
[23] J. Escobar, J.A. Toledo, M.A. Cortés, M.L. Mosqueira, V. Pérez, G. Ferrat, E. López-Salinas, E. Torres-García, Catal. Today 106 (2005) 222.
[24] S. Inoue, A. Muto, H. Kudou, T. Ono, Appl. Catal. A 269 (2004) 7.
[25] M. Houalla, N. Nag, A.V. Sapre, D.H. Broderick, B.C. Gates, AIChEJ 24 (1978) 1015.
[26] J. Mijoin, G. Pérot, F. Bataille, J.L. Lemberton, M. Breysse, S. Kasztelan, Catal. Lett. 71 (2001) 139.
[27] E.J.M. Hensen, P.J. Kooyman, Y. van der Meer, A.M. van der Kraan, V.H.J. de Beer, J.A.R. van Veen, R.A. van Santen, J. Catal. 199 (2001) 224.
[28] M. Daage, R.R. Chianelli, J. Catal. 149 (1994) 414.
[29] Y. Nishimura, T. Kameoka, T. Sato, Y. Yoshimura, H. Shimada, N. Matsubayashi, A. Nishijima, in: G. Poncelet, et al. (Eds.), Environmental Catalysis, SCI Pub., Roma, Italy, 1995, p. 403.
[30] F. Bataille, J.L. Lemberton, P. Michaud, G. Pérot, M. Vrinat, M. Lemaire, F. Schulz, M. Breysse, S. Kasztelan, J. Catal. 191 (2000) 409.
[31] G.C. Laredo, S. Leyva, R. Alvarez, M.T. Mares, J. Castillo, J.L. Cano, Fuel 81 (2002) 1341.
[32] I. Wang, R.C. Chang, J. Catal. 117 (1989) 266.
[33] J.G. Weissman, E.I. Ko, S. Kaytal, Appl. Catal. 94 (1993) 45.
[34] R.C. Chang, I. Wang, J. Catal. 107 (1987) 195.
[35] C.M. Lu, Y.-M. Lin, I. Wang, Appl. Catal. A 198 (2000) 223.